Band structure and Fermi surface of atomically uniform lead films

2010 New J. Phys. 12 113034

(http://iopscience.iop.org/1367-2630/12/11/113034)

New Journal of Physics
The open-access journal for physics

Band structure and Fermi surface of atomically uniform lead films

Shaolong He[1,2,8,9], Zhenhua Zeng[3,8,9], Masashi Arita[1], Masahiro Sawada[1,4], Kenya Shimada[1,4], Shan Qiao[5,9], Guoling Li[3], Wei-Xue Li[3,9], Yan-Feng Zhang[6], Yi Zhang[2], Xucun Ma[2], Jinfeng Jia[7], Qi-Kun Xue[7], Hirofumi Namatame[1,4] and Masaki Taniguchi[1,4]

[1] Hiroshima Synchrotron Radiation Center, Hiroshima University, Higashi-Hiroshima 739-0046, Japan
[2] Institute of Physics, Chinese Academy of Sciences, Beijing 100190, People's Republic of China
[3] State Key Laboratory of Catalysis, Dalian Institute of Chemical Physics, Chinese Academy of Sciences, Dalian 116023, People's Republic of China
[4] Graduate School of Science, Hiroshima University, Higashi-Hiroshima 739-8526, Japan
[5] Department of Physics, Advanced Materials and Surface Physics Laboratory, Fudan University, Shanghai 200433, People's Republic of China
[6] Institute of Multidisciplinary Research for Advanced Materials, Tohoku University, Japan
[7] Department of Physics, Tsinghua University, Beijing 100084, People's Republic of China
E-mail: shaolonghe@aphy.iphy.ac.cn, qiaoshan@fudan.edu.cn and wxli@dicp.ac.cn

New Journal of Physics **12** (2010) 113034 (9pp)
Received 18 July 2010
Published 17 November 2010
Online at http://www.njp.org/
doi:10.1088/1367-2630/12/11/113034

Abstract. Atomically uniform lead films are prepared on Si(111)-(7 × 7) substrates by the molecular beam epitaxy method, and their electronic structures are investigated by high-resolution angle-resolved photoemission spectroscopy and first-principles density functional theory calculations. We have observed the six-fold symmetric Fermi surfaces of Pb/Si(111)-(7 × 7) films. Their topology

[8] These authors contributed equally to this work.
[9] Authors to whom any correspondence should be addressed.

and size are almost the same regardless of the difference of film thicknesses (17, 21, 24 and 25 monolayers). The comparison between the measured and calculated thin-film Fermi surfaces suggests that the as-prepared Pb/Si(111)-(7 × 7) films are dominated by the hexagonal-close-packed stacking films instead of the face-centered-cubic ones. The theoretical calculations also indicate that spin–orbit coupling plays an important role in the band structures and Fermi surface topologies of Pb films.

Contents

1. Introduction

By using bottom-up and quantum engineering methods in nanoscience, a variety of novel properties and interesting physical phenomena have been discovered in low-dimensional materials that only recently have been produced in the laboratory (an example is graphene, [1]). Quantum size effects (QSEs) from the confinement and interference of electrons in nanostructures are substantial in both the formation and various novel physical properties of these nanomaterials, although control of the film morphology, to which electron interference is very sensitive, remains one of the most important technical challenges [2]–[7]. For investigations of QSEs, Pb ultrathin films grown on Si(111) surfaces served as an archetypal system because the Fermi wavelength is nearly four times the interlayer distance along the (111) crystallographic direction. This near-commensurability between the electronic and crystallographic length scales leads to an even–odd two-monolayer (ML) oscillation in the physical and chemical properties of Pb films on silicon, due to the presence of a quantum well state (QWS) formed in the ultrathin films [8]–[10]. In particular, it has been demonstrated unambiguously that the superconducting transition temperature of Pb/Si(111) films oscillates as a function of film thickness due to the modulation of the density of states at the Fermi level (E_F) by a QWS [11]–[14]. Such prominent modulation in physical properties and chemical reactivity by QSEs in Pb/Si(111) films is remarkable, and thus has attracted extensive theoretical and experimental research effort. The electronic structure is fundamentally important to understand the electronic transport and superconductivity of metallic films. Although several angle-resolved photoemission spectroscopy (ARPES) results on Pb ultrathin films have been reported [15]–[20], the Fermi surface (FS) topology is yet to be addressed.

In this paper, we report the growth of atomically uniform lead films on Si(111)-(7 × 7) surfaces and high-resolution ARPES studies on band dispersions and FSs of the as-grown films. The full FSs with six-fold symmetry have been elucidated for the first time, and their topology and size show no film thickness dependence for 17, 21, 24 and 25 MLs. A detailed comparison with the density functional theory (DFT) calculations suggests that the as-grown Pb/Si(111)-(7 × 7) films are dominated by hexagonal-close-packed (hcp) rather than face-centered-cubic

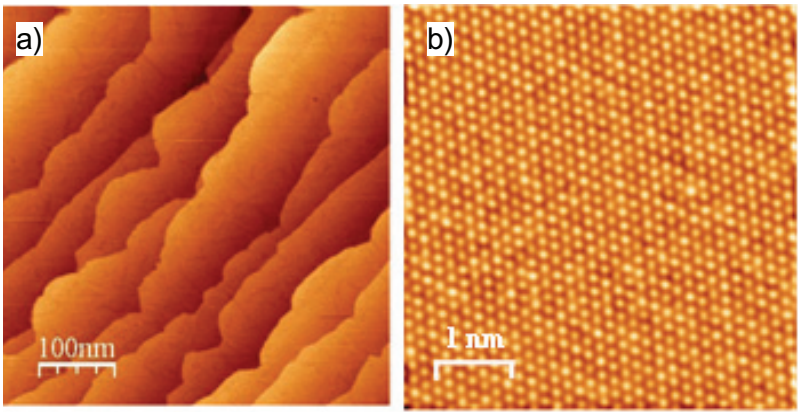

Figure 1. (a) Room-temperature STM topographic image (500 nm × 500 nm) of a perfect 21-ML Pb/Si(111)-(7 × 7) film. (b) Atomic-resolution STM image showing the Pb film surface as a close-packed structure with a lattice constant of 3.46 Å.

(fcc) stacking. DFT calculations also show that spin–orbit coupling (SOC) plays a significant role in the band structures and FS topologies of Pb films.

2. Experiment

The experiment was performed at Hiroshima Synchrotron Radiation Center (HSRC), Hiroshima University. Pb/Si(111)-(7 × 7) films with thicknesses of 17, 21, 24 and 25 MLs were prepared by evaporating lead on Si(111)-(7 × 7) surfaces at 100 K and were gradually annealed to room temperature. The evaporating rate was carefully adjusted to favor the (bi)layer-by-(bi)layer growth mode at 100 K, which was verified by scanning tunneling microscopy (STM) images and reflection high-energy electron diffraction patterns. Evaluation of the Pb/Si(111)-(7 × 7) film thicknesses with atomic-layer resolution by using STM and ARPES is the same as the method reported in previous studies [11, 12]. Films were then transferred to the analysis chamber with a base pressure of 5×10^{-11} Torr for *in situ* ARPES measurements. The ARPES spectra were taken by a VG Scienta-R4000 electron analyzer at beamline BL-9A of HSRC [21]. The energy resolution was set at $\Delta E = 12$ meV at a photon energy around 21 eV. The momentum resolution was set at $\Delta k = 0.007$ Å^{-1} for the high momentum resolution measurements and $\Delta k = 0.021$ Å^{-1} for the FS mapping.

The band structures and FSs of Pb films were calculated using the Vienna *ab initio* simulation package [22] with projector augmented wave potentials [23] and the generalized gradient approximation formulated by Perdew, Burke and Ernzerhof (GGA-PBE) for the exchange-correlation functional [24]. Pb 6s6p electrons were treated as valence electrons, and a kinetic energy cutoff of 100 eV was used for the expansion of the wavefunction. The SOC was included explicitly in the present calculations unless otherwise indicated. The surface Brillouin zone (SBZ) was sampled by a $(12 \times 12 \times 1)k$ point grid for fcc(111) and hcp(0001) (1 × 1) supercells. In this study, we have assumed a free-standing pure Pb slab of 21 MLs. The top five layers on either side of the slab were allowed to relax until the residual forces were less than 0.02 eV Å^{-1}, while the interior 11 layers were held at the optimized bulk lattice constant [25].

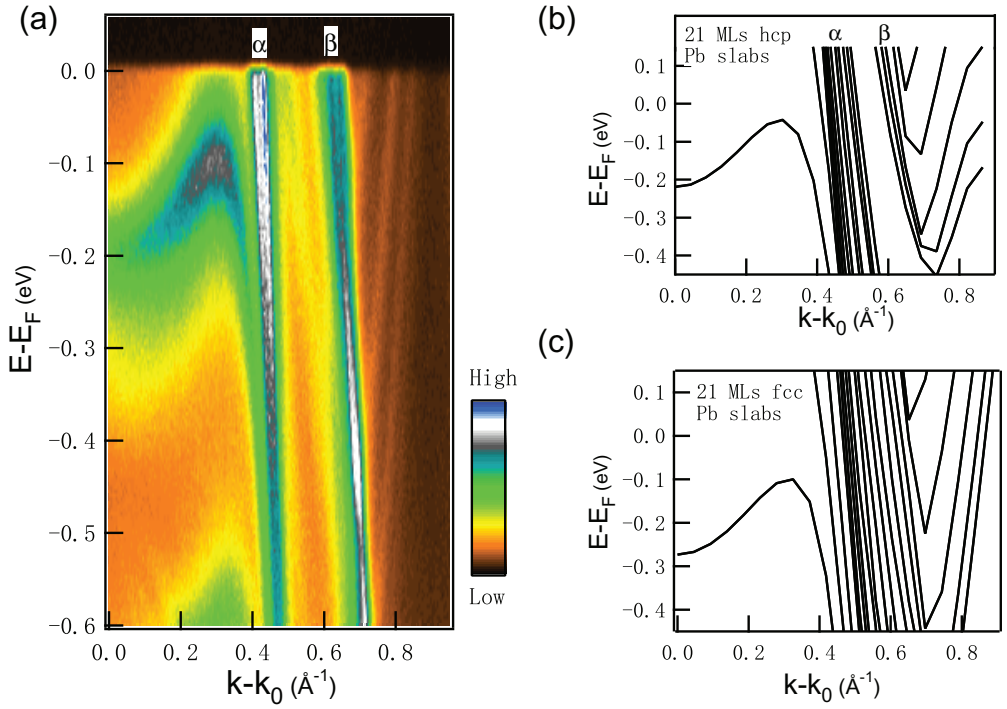

Figure 2. (a) ARPES intensity image of a 21-ML Pb/Si(111)-(7 × 7) film taken, at a temperature of 12 K, along the $\overline{\Gamma M}$ direction with a photon energy of 21 eV. (b) and (c) DFT calculated results for the 21-ML hcp and fcc stacking Pb slabs along $\overline{\Gamma M}$ after including SOC, respectively.

3. Results and discussion

Figure 1(a) presents a typical room-temperature STM image of a 21-ML Pb film on Si(111)-(7 × 7), showing highly uniform thickness of the film. Figure 1(b) presents an atomic-resolution STM image of the close-packed plane of the Pb film and further verifies an atomically flat surface. The in-plane lattice constant is estimated to be 3.46Å using STM data, which is the same as the Pb bulk value.

Figure 2(a) shows the ARPES intensity plot along $\overline{\Gamma M}$ obtained from a 21-ML Pb/Si(111)-(7 × 7) film at a photon energy of 21 eV. The dispersion of the QWS in this film is very similar to a previous ARPES study [15]. Near the $\overline{\Gamma}$ point of the SBZ, a sharp QWS peak around a binding energy of 0.2 eV can be resolved, which confirms the thickness uniformity and atomic smoothness of the films. Away from the $\overline{\Gamma}$ point, there are two separated bulk-derived bands labeled as α and β, with steep gradient cross E_F at $\mathbf{k} - \mathbf{k}_0 \sim 0.42$ and 0.65Å^{-1}, respectively. The α and β bands are well separated, and thus the two bands form a gap between them. The Fermi velocities of the α and β bands, defined as the slope of the dispersions at Fermi energy $v_F = (1/\hbar)(dE/dk)$, are evaluated as $v_{F\alpha} \approx 1.1 \times 10^6$ and $v_{F\beta} \approx 7.4 \times 10^5$ m s^{-1}, respectively.

In figures 2(b) and (c), the calculated band structures for the 21-ML hcp Pb(0001) and fcc Pb(111) films (by including SOC) are plotted. The observed gap between the α and β bands can be theoretically reproduced by assuming hcp stacking, not fcc stacking. According to the calculated band dispersions, we can see that neither the α nor the β band in figure 1(a)

represents a single band. Both of them actually consist of many sub-bands. For the hcp Pb film, the calculated Fermi velocities v_F are 1.1×10^6 and 7.3×10^5 m s^{-1} for the α and β bands, respectively, in excellent agreement with the experimental values. These observations suggest that the as-prepared films are dominated by the hcp stacking phase. Note that no gap was found even in hcp stacking when SOC was not included in the calculations. For fcc stacking, our calculations indicate that the SOC effect on band structure is modest along $\overline{\Gamma M}$ and significant along $\overline{\Gamma K}$. Note that the calculated band structure of the hcp Pb bulk crystal shows a similar gap with the inclusion of SOC, which indicates that the features observed here are not restricted to the surface-derived states. These results highlight the importance of SOC on the band structures of Pb films, which was also reported in previous studies of Pb films [17, 26]. As shown below, the gap between the α and β bands is also crucial to the measured FS topology.

Figures 3(a)–(d) show the FS maps of the 17-, 21-, 24- and 25-ML Pb/Si(111)-(7 × 7) films obtained from high-resolution ARPES data taken at a photon energy of 21 eV and integrated over the energy window $E_F \pm 5$ meV. We found that the size and topology of these FSs are nearly the same regardless of the different film thicknesses. The observed FSs centered around the $\overline{\Gamma}$ point show a clear six-fold symmetry and are different from that of bulk fcc Pb(111), which has three-fold symmetry at the Γ and L points [27].

Near the zone center, the experimental FS features can be seen as the superposition of two crossing triangular FSs of fcc Pb(111) at the Γ point. Then the observed FSs of Pb films may be simply the superposition of two triangular FS features derived from two fcc stacking domains, which are rotated 60° apart from each other. This possibility can be excluded by measuring the 21-ML Pb/Si(111)-(7 × 7) film's band dispersion along the red line sketched in figure 4(a), which is close to the cross point of the two triangular FSs. The measured band dispersions were presented in figure 4(b) and the corresponding energy distribution curves (EDCs) are shown in figure 4(c). A simple band overlap of two domains should result in an intensity increase near the cross point, which is obviously not the case here. Instead, a gap exists in the cross region, as evidenced from two well-separated peaks in the EDCs (figure 4(c)). This observation rules out the possibility of two domains and indicates the existence of band interaction.

In figure 3(e), we show the calculated FS considering the SOC of a 21-ML fcc Pb film, which clearly shows six-fold symmetry and is consistent with a previous theoretical calculation [20]. The calculated FS without SOC on the fcc Pb film (not shown) is found to be nearly the same as the one including SOC in figure 3(e), and neither of them is consistent with the measured FS. On the other hand, we found that SOC does affect the FS topologies of hcp Pb films, as shown in figure 3(f) (without SOC) and (g) (with SOC). We should note that only the calculated hcp FS after including SOC matches the experiment very well. We also calculated the FSs of Pb slabs with mixed fcc and hcp stacking (not shown). The results show a simple superposition of the corresponding fcc (figure 3(e)) and hcp (figure 3(f)) stacking FSs, which cannot explain the sharp features of measured FSs. The perfect agreement between measured and calculated FSs on the hcp stacking film including SOC suggests that the as-prepared Pb/Si(111)-(7 × 7) films are dominated by the hcp stacking phase instead of the fcc one [28]–[31].

The calculations also show that SOC plays an important role in the band structures and FS topologies of Pb films. This can be further seen by comparing with the measured band dispersion shown in figure 4, where the noncrossing gap near the cross point of the two triangular FS features is studied. To determine the gap size, we fitted the corresponding EDCs in figure 4(c) after subtracting a suitable background and obtained the band position shown as filled circles in

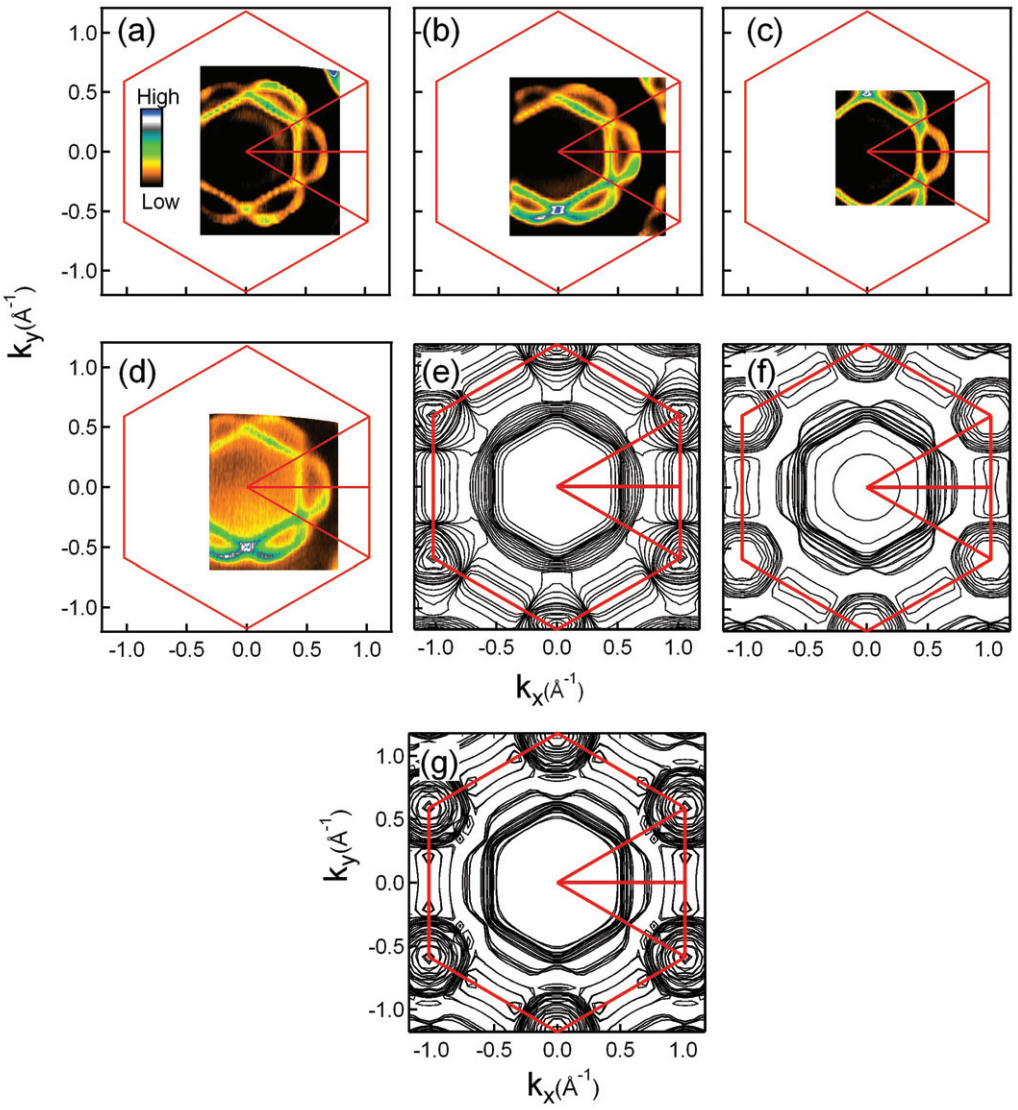

Figure 3. (a)–(d) Integrated ARPES spectral weight close to the Fermi level on the 17-, 21-, 24- and 25-ML Pb/Si(111)-(7 × 7) films at a photon energy of 21 eV. The SBZ of a Pb(0001) surface is indicated by a solid red line. (e) Calculated FSs on the 21-ML fcc Pb(111) film considering SOC. Calculated FSs on 21-ML hcp Pb(0001) films without SOC (f) and with SOC (g).

figure 4(b). The gap size is thus determined to be about 270 meV and is close to the calculated value on the hcp Pb(0001) film after the inclusion of SOC. We therefore expect that the strong SOC effect identified here can be explored further by spin-resolved ARPES experiments [26].

From the measured and calculated (hcp) FS, there are two separated closed contours centered around the $\overline{\Gamma}$ point, namely, a hexagonal hole pocket A and a snowflake-shaped hole pocket B, as sketched in figure 4(a). The two closed contours A and B are associated with the α and β bands indicated in figures 2(a) and (b). For the band structures along $\overline{\Gamma K}$, we found that both the measured (figures 3(a)–(d)) and calculated (figure 3(g)) Fermi wave vectors

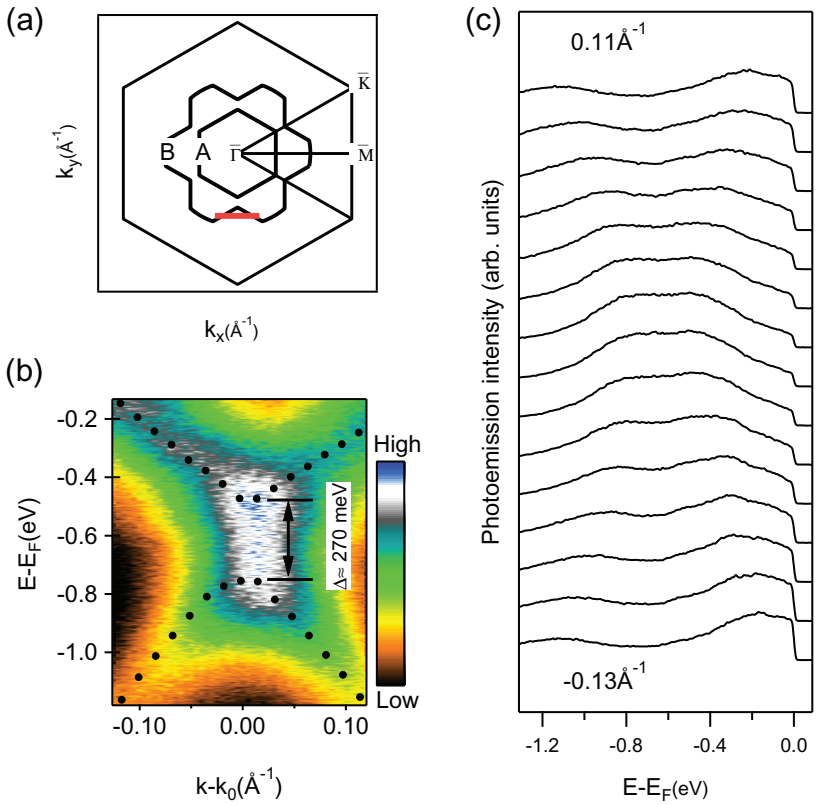

Figure 4. (a) A sketch of the Pb film's FS features centered at the $\bar{\Gamma}$ point. (b) The band intensity map, obtained on the 21-ML Pb/Si(111)-(7 × 7) film, near the crossing point along the red line in (a). (c) EDCs for selected k points along the red line in (a). The filled circles in (b) indicate the peak positions in the EDCs.

of the hole pocket A are smaller than those of the hole pocket B, which separates contours A and B further.

The fine FS topologies obtained from the high-resolution ARPES measurements on Pb/Si(111)-(7 × 7) films allow detailed comparison between the experiment and DFT calculations. Our results suggest that the as-grown Pb/Si(111)-(7 × 7) films are dominated by the hcp stacking phase. On the other hand, the previous surface x-ray diffraction studies indicated that the Pb film grown on the Pb/Si(111)-$\sqrt{3} \times \sqrt{3}R30^\circ$ surface possesses fcc structure [28, 30, 31]. The different substrate structures may account for the formation of the different structures of Pb films due to the substrate effects [32]. In fact, the optimized in- and out-plane equilibrium lattice constants for fcc Pb(111) and hcp Pb(0001) films are nearly the same and the difference is less than 0.02 Å, whereas the difference in total energies is less than 10 meV/Pb atom. These facts then imply that even subtle differences in substrate structure or growth dynamics may result in different Pb film structures, and therefore rationalize the formation of the hcp Pb film on the Si(111)-(7 × 7) surface and that of the fcc Pb film on the Pb/Si(111)-$\sqrt{3} \times \sqrt{3}R30^\circ$ surface. Most of the QSEs on Pb/Si(111) films observed so far, however, may not be affected by the hcp stacking Pb(0001) films since both their Fermi wavelength and interlayer spacing, which are critical to various even–odd oscillations with

respect to the thickness of the films, are essentially the same as those of the fcc stacking Pb(111) films. The structural difference between fcc and hcp stacking occurs at the second nearest neighbor and corresponding symmetries. The physical properties involved with them would be expected to be modified. As mentioned above, SOC affects pronouncedly the band structure of hcp Pb(0001) films along the $\overline{\Gamma M}$ direction, and of fcc Pb(111) films along $\overline{\Gamma K}$. We also expect that phonon spectra and electron–phonon coupling of the hcp Pb films would be very different from the fcc ones.

4. Conclusion

In conclusion, the electronic structures of atomic-layer-resolved Pb films grown on Si(111)-(7×7) have been explored by high-resolution ARPES and DFT calculations. We observed the six-fold symmetric FSs for as-prepared films. Major FS features, including topology and size, are not dependent on film thickness (17, 21, 24 and 25 MLs). The comparison between the measured and calculated results suggests that as-prepared Pb/Si(111)-(7×7) films are dominated by hcp rather than fcc stacking. We also found that the spin–orbit interaction is essential to FS topologies and band structures. In order to further verify this study, we need *in situ* structure measurements of Pb/Si(111)-(7×7) films over a wide thickness range and wide growth conditions.

Acknowledgments

We thank X J Zhou and A Stierle for fruitful discussions. The synchrotron radiation experiments were performed under the approval of HSRC (Proposal No. 07-A-66). SLH was supported by NSFC (10974239). SQ was supported by Shanghai Pujiang program (10979021) and NSFC (11027401). WXL and XCM were supported by NSFC (20733008, 20873142) and the National Basic Research Program of China (2007CB815205).

References

[1] For a review, see Geim A K *et al* 2007 *Nat. Mater.* **6** 183
[2] Zhang Z Y *et al* 1998 *Phys. Rev. Lett.* **80** 5381
[3] Jia Y *et al* 2006 *Phys. Rev.* B **74** 035433
[4] Budde K *et al* 2000 *Phys. Rev.* B **61** R10602
[5] Mans A *et al* 2002 *Phys. Rev.* B **66** 195410
[6] Hong H *et al* 2003 *Phys. Rev. Lett.* **90** 076104
[7] Qin S *et al* 2009 *Science* **324** 5932
[8] For a review, see Chiang T C 2000 *Surf. Sci. Rep.* **39** 181
[9] Jia J F *et al* 2007 *J. Phys. Soc. Japan* **76** 082001
[10] Ma X *et al* 2007 *Proc. Natl Acad. Sci. USA* **104** 9204
[11] Guo Y *et al* 2004 *Science* **306** 1915
[12] Zhang Y F *et al* 2005 *Phys. Rev. Lett.* **95** 096802
[13] Özer M M *et al* 2006 *Nat. Phys.* **2** 173
[14] Özer M M *et al* 2007 *Science* **316** 1594
[15] Upton M H *et al* 2005 *Phys. Rev.* B **71** 033403
[16] Dil J H *et al* 2006 *Phys. Rev.* B **73** 161308
[17] Dil J H *et al* 2007 *Phys. Rev.* B **75** 161401

[18] Kirchmann P S *et al* 2007 *Phys. Rev.* B **76** 075406
[19] Mathias S *et al* 2010 *Phys. Rev.* B **81** 155429
[20] Miyata N *et al* 2008 *Phys. Rev.* B **78** 245404
[21] Arita M *et al* 2002 *Surf. Rev. Lett.* **9** 535
[22] Kresse G *et al* 1996 *Phys. Rev.* B **54** 11169
[23] Kresse G *et al* 1999 *Phys. Rev.* B **59** 1758
[24] Perdew J P *et al* 1996 *Phys. Rev. Lett.* **77** 3865
[25] Liu X *et al* 2008 *Appl. Phys. Lett.* **93** 093105
[26] Dil J H *et al* 2008 *Phys. Rev. Lett.* **101** 266803
[27] Anderson J R and Gold A V 1965 *Phys. Rev.* A **139** 1459
[28] Czoschke P *et al* 2003 *Phys. Rev. Lett.* **91** 226801
[29] Mans A *et al* 2005 *Phys. Rev.* B **72** 155442
[30] Czoschke P *et al* 2005 *Phys. Rev.* B **72** 035305
[31] Czoschke P *et al* 2005 *Phys. Rev.* B **72** 075402
[32] Dil J H *et al* 2010 *J. Phys.: Condens. Matter* **22** 135008